PAPER

Supramolecular liquid crystalline dendrimers with a porphyrin core and functional carboxylic acid dendrons†

Alberto Concellón,[a] Madalina Bucoş,[a] José Luis Serrano,[b] Pilar Romero*[a] and Mercedes Marcos*[a]

Novel liquid crystalline porphyrin dendrimers derived from 5,10,15,20-tetra-(4-pyridyl)porphyrins (**TPyP**) and their Zn complexes (**ZnTPyP**) have been synthesized by hydrogen bonding between the porphyrin core and four peripheral carboxylic acid dendrons derived from bis(hydroxymethyl)propionic acid (bis-MPA) to obtain 4 : 1 complexes. One family is derived from symmetric dendrons (*G* = 1 and 2) bearing promesogenic units in the terminal positions and two other families are derived from asymmetric dendrons (*G* = 1) that combine the promesogenic unit and an active moiety derived from coumarin or pyrene units. The formation of the complexes was confirmed by IR and NMR spectroscopy. The liquid crystalline properties were investigated by differential scanning calorimetry, polarizing optical microscopy and X-ray diffraction. Only porphyrin dendrimers (free base and Zn complexes) derived from symmetric dendrons exhibited a SmC mesophase. Porphyrin dendrimers derived from asymmetric dendrons did not show liquid crystalline behaviour. The UV-vis absorption and emission properties of the porphyrin dendrimers containing coumarin or pyrene have been investigated.

Introduction

Dendrimers are highly branched macromolecules that are almost monodisperse and this is an important difference to most other synthetic polymers, which are polydisperse.[1–6] The interest in these compounds is due to the special structural characteristics, which give them unique properties. Dendrimers can be obtained by divergent or convergent iterative methods[7] but an alternative strategy is based on supramolecular chemistry, which allows the preparation of dendrimers by a self-assembly process based on non-covalent interactions, such as metal coordination chemistry, hydrogen-bonding or electrostatic interactions.[8]

In addition, when dendrimers are functionalised with promesogenic units they can self-organise into liquid crystal phases. Liquid crystal dendrimers represent an attractive option for the design of functional materials that retain the inherent properties of dendrimers and provide well-organised materials that are able to respond to external stimuli.[9–15]

In 1998 Lehn and Zimmerman *et al.* reported the preparation of a dendrimer consisting of three H-bonded dendrons of disubstituted phthalhydrazide units, which self-organised to give a thermotropic discotic liquid crystal.[16] Since then, several papers have been published on supramolecular liquid crystal dendrimers obtained by the self-assembly of dendrons.[17]

We recently studied a new type of liquid crystal dendrimers functionalised with carbazole, coumarin and pyrene groups as fluorescence moieties.[18,19] These compounds were prepared by hydrogen bonding between a triazine core (**M**), as an electron-transporting unit, and three peripheral carboxylic acid bifunctionalised dendrons derived from bis(hydroxymethyl)propionic acid (bis-MPA).

As a continuation of our research programme in this area, we synthesised and characterised three novel families of compounds that were formed by hydrogen bonding between 5,10,15,20-tetra(4-pyridyl)porphyrin (**TPyP**) or zinc metalated porphyrin (**ZnTPyP**) as the core and four peripheral bifunctionalised dendrons derived from bis(hydroxymethyl)propionic acid (bis-MPA), which were described in a previous paper.[19] The **TPyP** unit was selected for this work due to its ability to recognise other molecules through the donation and acceptance of hydrogen bonds,[20,21] a characteristic that plays a key role in the self-organisation of molecules and thus facilitates the formation of liquid crystals in low molecular weight compounds as well as in polymers or dendrimers. Zinc complexes of porphyrin dendrimers have been prepared with the aim of increasing the stability and providing better photophysical properties compared to free-base porphyrins. Coumarin and pyrene were chosen as the fluorophores in the dendrimer. Pyrene is a widely

[a]*Instituto de Ciencia de Materiales de Aragón, Universidad de Zaragoza-CSIC, 50009 Zaragoza, Spain. E-mail: mmarcos@unizar.es; promero@unizar.es*

[b]*Departamento de Química Orgánica, Facultad de Ciencias, Instituto de Nanociencia de Aragón, Universidad de Zaragoza, 50009 Zaragoza, Spain*

† Electronic supplementary information (ESI) available. See DOI: 10.1039/c6ra13604d

used probe due to its high fluorescence efficiency and excimer formation[22,23] and coumarin is biocompatible and is highly valuable as a fluorescent chemosensor in a variety of fields.[24–26]

The structures of the porphyrin dendrimers and dendrons are shown in Scheme 1.

Results and discussion

Synthesis of dendrons

Carboxylic acid dendrons were prepared by esterification with dicyclohexylcarbodiimide (DCC) of the monomer 2,2-bis(hydroxymethyl)propionic acid (bis-MPA), protected with a benzyl
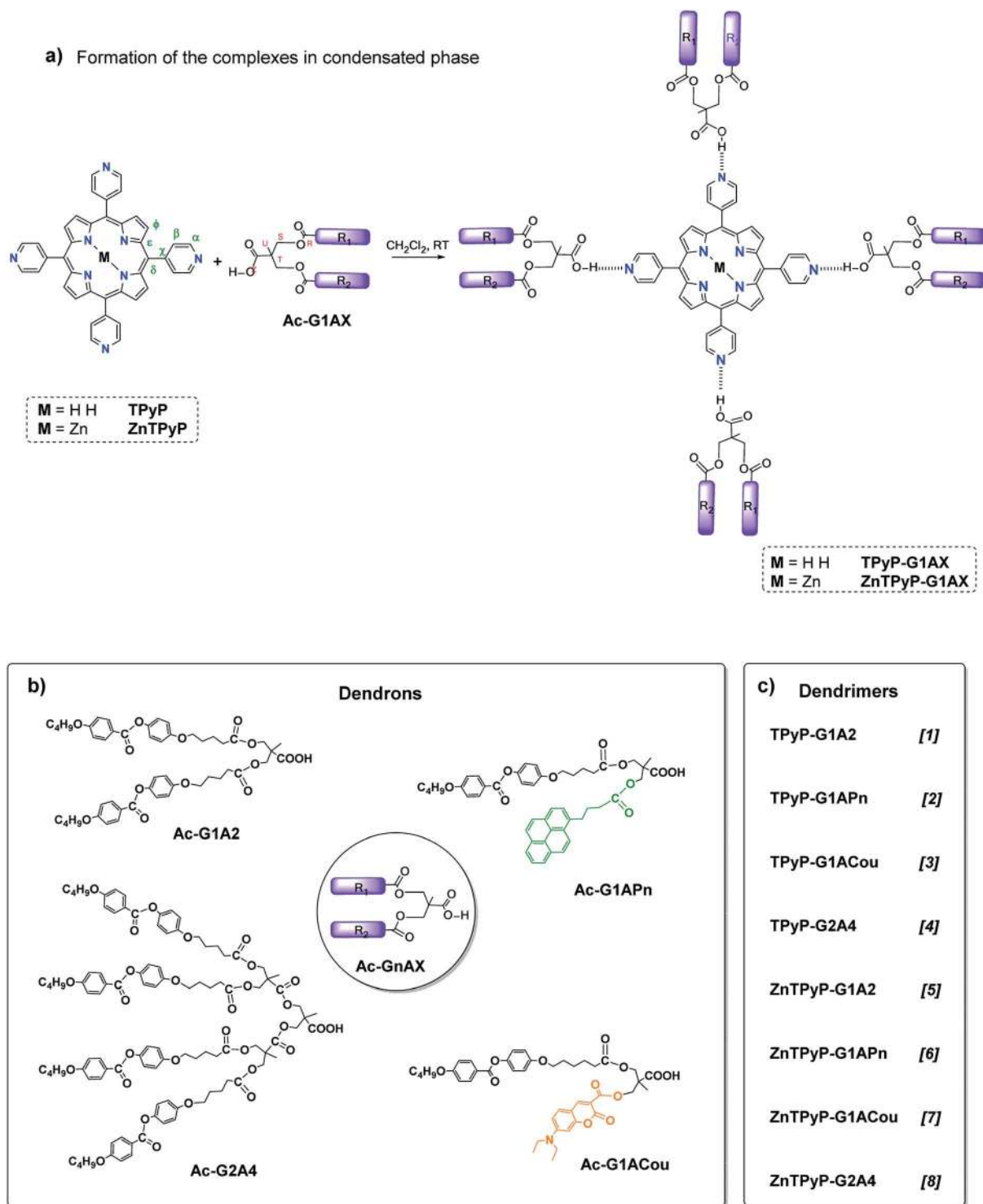
Scheme 1 Schematic representation of: (a) synthetic route and atom labels for the first generation of dendrimer complexes **TPyP-G1AX** and **ZnTPyP-G1AX**, (b) carboxylic acid dendrons of the first (**Ac-G1AX**) and second (**Ac-G2A4**) generation, (c) nomenclature of the supramolecular dendrimers.

ester group, and the appropriate promesogenic acid by previously reported method.[19]

Typical procedure for the synthesis of the dendrimers derived from porphyrins and metalloporphyrins

The hydrogen-bonded complexes were prepared by mixing a dichloromethane (CH$_2$Cl$_2$) solution of the appropriate amount of each component [5,10,15,20-tetra(4-pyridyl)porphyrin (**TPyP**) or Zn(II) 5,10,15,20-tetra(4-pyridyl)porphyrin (**ZnTPyP**) and the dendron carboxylic acid derivative in a 1 : 4 ratio] and slowly evaporating the solvent by stirring at room temperature. The general synthetic route for the dendrimers is shown in Scheme 1.

Full characterization data for all dendrimers are provided in the ESI.†

Structural characterization

The formation and stability of intermolecular H-bonding associations between the **TPyP** or **ZnTPyP** and the dendrons were studied by infrared spectroscopy (FTIR) on neat samples as KBr pellets and by Nuclear Magnetic Resonance (NMR) spectroscopy on solutions in deuterated solvents. The results confirmed the proposed structures of these materials. The data are gathered in the ESI.†

NMR characterization

The chemical structures of the dendrimers were confirmed by one-dimensional ^{1}H and ^{13}C NMR spectroscopy and by two-dimensional ^{1}H–^{1}H COSY, ^{1}H–^{13}C HSQC and ^{1}H–^{13}C HMBC experiments. NMR signal assignments are gathered in the ESI (Fig. S1–S19†). For some dendrimers DOSY and ^{1}H–^{1}H NOESY spectra were also acquired. NMR signal assignments are provided in the ESI.†

Expansions of the ^{1}H and ^{13}C spectra of some dendrimers are shown in Fig. 1 and 2 along with those their dendrons and cores. The largest shifts in the dendron part are related to the
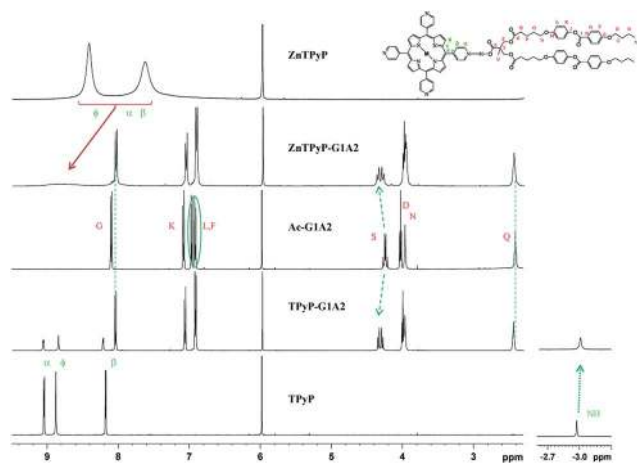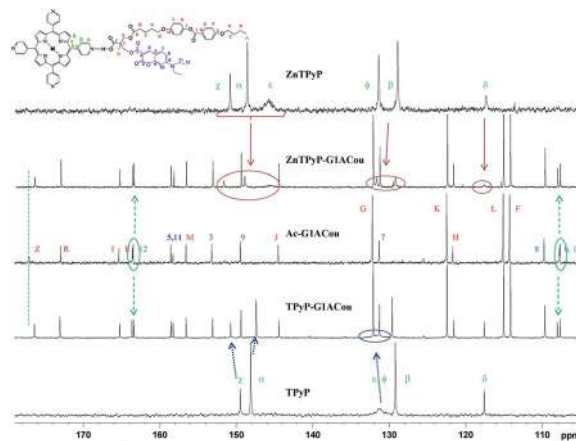

Fig. 2 Expansions of ^{13}C NMR spectra of complexes **TPyP-G1ACou** and **ZnTPyP-G1ACou** related to their dendron and porphyrin core (125 MHz, C$_2$D$_2$Cl$_4$, 25 °C).

nuclei nearest to the H bonds, as discussed in a previous publication.[19]

Thus, the shift and the change in the shape of the diastereotopic methylene (H$_S$, see Scheme 1) signals after H-bonding are particularly marked: H$_S$ protons are deshielding 0.08 ppm in both complexes with regard to acid **Ac-G1A2**, and the methyl H$_U$ signal are also deshielding (see Fig. 1). The aromatic protons of mesogenic units evidence shielding in the complexes. On the other hand, H$_\phi$ and NH protons of the **TPyP** core are shielding in 0.03 ppm. The NH and H$_\phi$ protons of protons of the **ZnTPyP** part in the complexes are broadened by several ppm (Fig. 1). In the ^{13}C NMR spectra the main shifts are evidenced by the –COOH (C$_Z$, see Scheme 1) and the methyl and methylene groups of bis-MPA (C$_U$ and C$_S$, see Scheme 1). Thus, for complexes derived from coumarin dendrons, after complexation the ^{13}C signals of the carboxylic acid are shielding 0.7 ppm and δ(^{13}C) of **TPyP** and **ZnTPyP** are different from the starting cores (see Fig. 2).

DOSY studies can also help to determine whether the hydrogen bonding interactions are formed between the dendron and the porphyrin core. When the complex components diffuse as a single molecular entity and have the same diffusion coefficient this provides evidence that a strong complex is formed. In the case where there is no interaction the diffusion coefficients of partners will remain the same as in their free states.[27] It can observe in Fig. S17 (see ESI†) that there is only one diffusion coefficient for this material and this is consistent with the presence of the complex **TPyP-G2A4** in C$_2$D$_2$Cl$_4$ solution.

Likewise, the stoichiometry of these complexes was determined by the Job's plot method and it was concluded that in solution the molecules are in 1 : 1 ratio (see ESI, Fig. S18†). However, ^{13}C CPMAS spectroscopy confirmed the formation of dendrimers with a 4 : 1 stoichiometry in the condensed phase. As a representative example the spectrum of **TPyP-G1A2** is shown in Fig. 3 along with those of the starting materials.
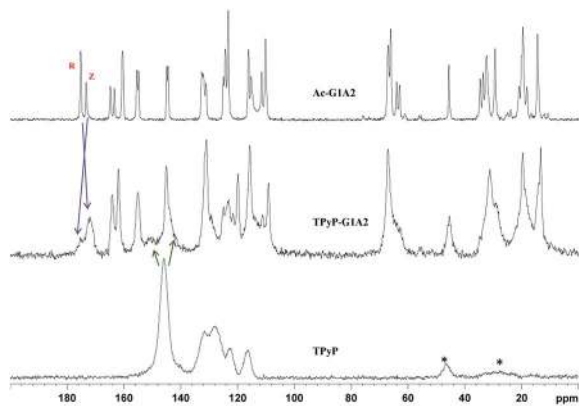

Fig. 1 Expansions of ^{1}H NMR spectra of complexes **TPyP-G1A2** and **ZnTPyP-G1A2** related to their dendron and porphyrin core (125 MHz, C$_2$D$_2$Cl$_4$, 25 °C).

Fig. 3 ^{13}C-CPMAS spectra of: dendron **Ac-G1A2** (top), **TPyP-G1A2** dendrimer (middle) and **TPyP** porphyrin (bottom).

Thermal stability of the dendrimers and dendrons

The thermal stabilities of the dendrimers were studied by thermogravimetric analysis (TGA) under a nitrogen atmosphere. All of the studied compounds exhibited good thermal stability and in all cases the 5% weight loss point was detected at temperatures higher than the isotropization process. The thermal analysis data are gathered in Table 1.

Liquid crystalline properties and XRD characterization

The mesomorphic behaviour of the compounds was analysed by polarized optical microscopy (POM), differential scanning calorimetry (DSC) and X-ray diffraction (XRD). Three cycles were carried out in DSC experiments and data were taken from the second cycle. It is worth noting that the DSC thermograms of these dendrimers are perfectly reproducible after the second

and subsequent heating–cooling cycles. In some cases, the clearing temperatures were taken from POM observations because transition peaks were not detected in DSC curves. Data for the porphyrin dendrimers synthesized are gathered in Table 1.

The liquid crystal phases were identified by POM observations. Porphyrin dendrimers derived from 5-[4-(4-butoxybenzoyloxy)phenyloxy]pentanoic acid (**TPyP-G1A2**, **ZnTPyP-G1A2**, **TPyP-G2A4** and **TPyP-G2A4**) showed textures compatible with a smectic C mesophase. Not homeotropic domains could be obtained in a temperature range when the sample was submitted to mechanical stress, supporting that the mesophase was smectic C and this was confirmed by X-ray diffraction. DSC traces corresponding to the second scan of **TPyP-G2A4** and the POM texture of **TPyP-G2A4** in the SmC mesophase taken at room temperature are shown in Fig. 4b.

Dendrimers derived from pyrene and coumarin were not mesomorphic (Table 1) but on heating the appearance of small red-coloured particles was observed. These particles could only be seen without polarized light and were not apparent under crossed polarizers. This observation suggests that the H-bond is broken as the temperature increases.

Comparison of the liquid crystal properties of dendrimers with the liquid crystal properties of the dendrons shows that the dendron and porphyrin dendrimer of the second generation **Ac-G2A4**, **TPyT-G2A4** are slightly more stable than the first generation analogues derived from dendron acid **Ac-G1A2**, but the mesomorphic properties are very different. Whereas acid dendron **Ac-G1A2** shows SmC and SmA (g 3 SmC 75 SmA 81 I)[19] and **Ac-G2A4** shows SmC and N (g 10 SmC 91 N 94 I) phases, porphyrin dendrimers only exhibit a SmC mesophase (Table 1).

In contrast to the above, pyrene (**Ac-G1APy**: g 14 N 90 I)[19] and coumarin (**Ac-G1ACou**: g 12 N 50 I)[19] dendrons show a nematic

Table 1 Thermal stability, mesogenic properties and XRD data for the dendrimers

Compound	$T_{5\%}{}^a$ (°C)	Thermal properties^b (T [°C], (ΔH [kJ mol^{-1}]))	d_{obs} (Å)	Phase	Structural parameters^c
TPyP-G1A2	275	g 14 C 41 SmC 54 (9.0) I	44.0	SmC	$d = 44.0$ $S = 154.7$ $S_{\text{ch}} = 38.7$
TPyP-G2A4	217	g 6 SmC 68 (17.5) I	44.0	SmC	$d = 44.0$ $S = 300.9$ $S_{\text{ch}} = 37.6$
TPyP-G1APn	248	—^{d}	—	—	—
TPyP-G1ACou	171	—^{d}	—	—	—
ZnTPyP-G1A2	242	g 80 SmC 88 (6.7) I	44.2	SmC	$d = 44.2$ $S = 156.4$ $S_{\text{ch}} = 39.1$
ZnTPyP-G2A4	166	g 13 SmC 69 (18.1) I	43.5	SmC	$d = 43.5$ $S = 307.0$ $S_{\text{ch}} = 38.4$
ZnTPyP-G1APn	213	—^{d}	—	—	—
ZnTPyP-G1ACou	226	—^{d}	—	—	—

^{a} Temperature at which 5% of the initial mass is lost. ^{b} Data obtained by DSC in the second heating process and taken at the maximum of the peak obtained at 10 °C min^{-1}. g = glass; SmC = smectic C mesophase; I = isotropic liquid. ^{c} d = layer spacing of the smectic phase (Å), S = estimated molecular cross-sectional area (Å^2), S_{ch} = estimated cross-sectional area per chain (Å^2). ^{d} LC properties were not observed.
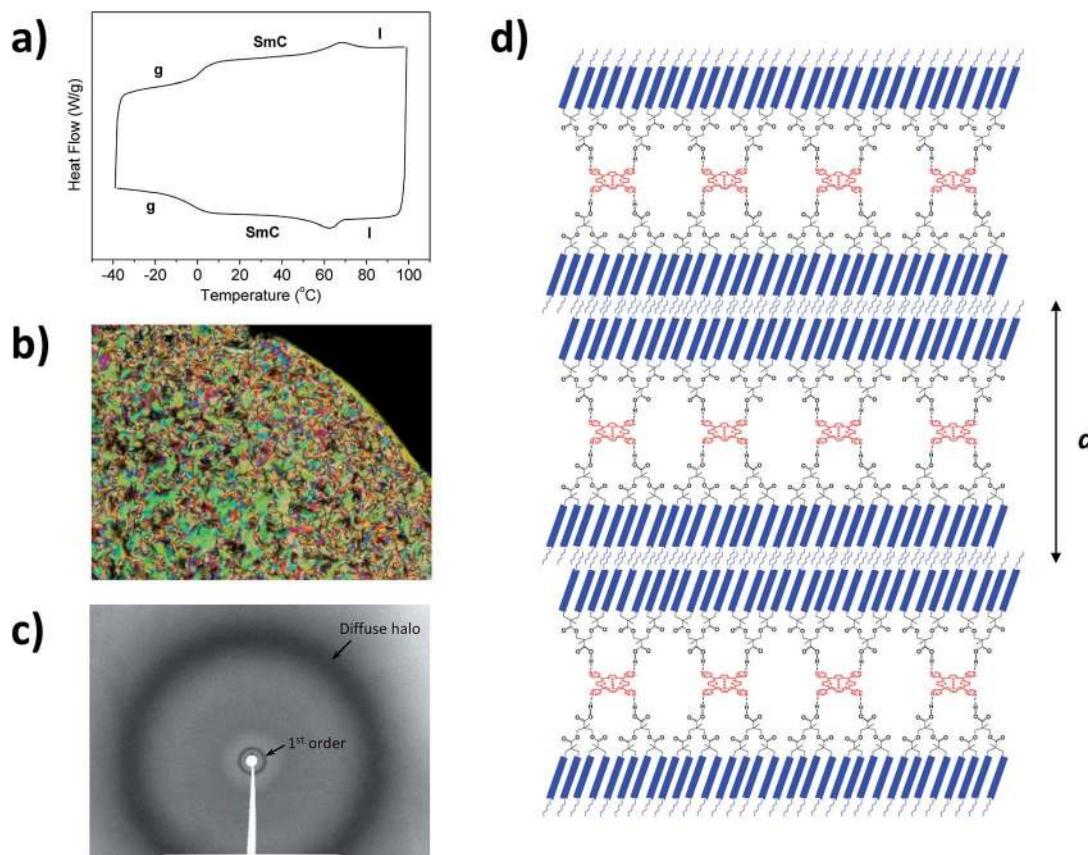
Fig. 4 (a) DSC traces corresponding to the second scan of **TPyP-G2A4** (10 °C min^{-1}; Exo down). (b) POM texture of **TPyP-G2A4** in the SmC mesophase taken at room temperature. (c) Room temperature XRD pattern of **TPyP-G2A4** in the SmC mesophase. (d) Proposed arrangement of **TPyP-G2A4** in the SmC mesophase.

phase. However, as mentioned before, the porphyrin derivatives of these functional dendrons do not show mesophases (see Table 1).

Comparison of the mesogenic behaviour of porphyrins of G = 1, **TPyP-G1A2** and **ZnTPyP-G1A2**, indicates that the Zn complex has a mesophase with a broad temperature range. It can be suggested that the presence of the metal in this porphyrin favours the mesogenic properties. However, in porphyrins of G = 2, **TPyP-G2A4** and **ZnTPyP-G2A4**, the mesophase temperature range is similar; in this case the metal does not appear to have an influence on the mesogenic properties of the porphyrin dendrimers. Similar behaviour was observed concerning the stability of the materials.

Mesophase formation was not observed for Zn-containing dendrimers derived from pyrene and coumarin (**ZnTPyP-G1APn** and **ZnTPyP-G1ACou**) but, as with the porphyrin without a metal, some particles were observed in the isotropic liquid.

A columnar phase was not observed for any of the liquid crystal porphyrin dendrimers synthesized in this study and this was unexpected taking into account the disk-shape of the porphyrin core. Only a smectic phase was observed for these materials.

The DSC traces corresponding to the second scan of the liquid crystalline porphyrin dendrimers and microphotographs of optical textures are collected in Fig. S23–S25.†

Powder XRD studies were performed at room temperature in order to confirm the nature of the mesophase and to determine the structural parameters. The data are gathered in Table 1. In all cases the diffraction pattern includes a diffuse halo in the high-angle region and one sharp, strong maximum in the small-angle region (see Fig. 4c as a representative example). This maximum is assigned to the first order reflection of the smectic layers and the layer spacing was deduced by applying Bragg's law. The diffuse halo is related to the conformational disorder of the liquid-like carbon chains. This kind of pattern corresponds to a smectic C organization on the basis of the optical textures and the structural parameters deduced from the XRD measurements.

The supramolecular complexes consist of four dendrons that surround the porphyrin core, with two of these dendrons oriented in two opposite directions and tilted with respect to the smectic layer (see Fig. 4d as a representative example). Thus, in the smectic mesophase the molecules of **TPyP-G1A2** and **ZnTPyP-G1A2** and the molecules of **TPyP-G2A4** and **ZnTPyP-G2A4** contain, respectively, four or eight mesogenic units in each direction. Furthermore, the layer spacing of the first generation complexes is similar to the layer spacing of the second generation complexes, thus confirming this kind of smectic C arrangement, which is similar to that previously found for H-bonded dendrimers prepared with the same dendrons and a melamine central core.[19]

The experimentally measured layer spacing (d) for the supramolecular complexes is shorter than the length in their most extended conformation (73 Å and 85 Å for the first and second generation dendrimers, respectively). This is due to a combination of two phenomena: the tilt in the smectic mesophase, and the interdigitation of the chains. Furthermore, it should be pointed out that the measured layer spacing is similar for the $G = 1$ and $G = 2$ dendrimers. This is expected considering that upon increasing the generation, the dendritic branches expand in the direction of the smectic plane, producing a broadening of the molecule without a significant increase in length.

Additional support for this structural model can be obtained by simple cross-section calculations. The molecular cross-sectional area (S) in Å^2 in a smectic mesophase can be calculated as: $S = M \times 10^{24}/d \times N_A$, where M is the molecular mass in g mol^{-1}, d is the experimentally measured layer spacing in Å, and N_A is Avogadro's number. This gives the estimated S values listed in Table 1. By dividing these values by the number of mesogenic units (or chains) oriented in each direction, we obtain the cross-sectional area per chain S_{ch}. The S_{ch} values of around 38–39 Å are too large for an orthogonal (smectic A) mesophase.[19,28]

It is noteworthy that *a priori* the molecular structure of the supramolecular dendrimers seems to induce a discotic arrangement, although the flexibility of the bis-MPA units allows the formation of a calamitic superstructure, as proposed in the model suggested by the XRD studies.

Optical properties

The UV-vis absorption spectra of dendrimers containing pyrene and coumarin were measured in dilute dichloromethane solution. Fluorescence spectra in dichloromethane solution were only recorded for derivatives containing pyrene and coumarin chromophores. All UV-vis spectra of the synthesised dendrimers derived from **TPyP** show a typical porphyrinic spectrum with four weak Q-bands between 500 and 700 nm and an intense Soret (B) near 420 nm. The absorption bands of the Zn-metallodendrimers decrease in intensity and this is attributed to the increase in symmetry of these complexes. Furthermore, pyrene and coumarin complexes showed the characteristic absorption bands of their chromophore units: two bands at about 262 and 425 nm typical of the coumarin and several bands with maxima at 266, 277, 328 and 344 nm for pyrene dendrimers.

The emission spectra of coumarin-containing dendrons in solution after excitation at $\lambda_{max} = 262$ nm display a band at 456–457 nm and this is related to the luminescence of the coumarin unit, while the florescence spectra of pyrene dendrimers contain bands at 377 and 398 nm after irradiation at 277 or 345 nm. The emission spectra of all dendrimers after excitation in the Soret band revealed strong red fluorescence with a maximum at around 600–650 nm.

The optical data for pyrene and coumarin dendrimers are collected in Table S1† and absorption and emission spectra of these compounds are shown in Fig. 5.
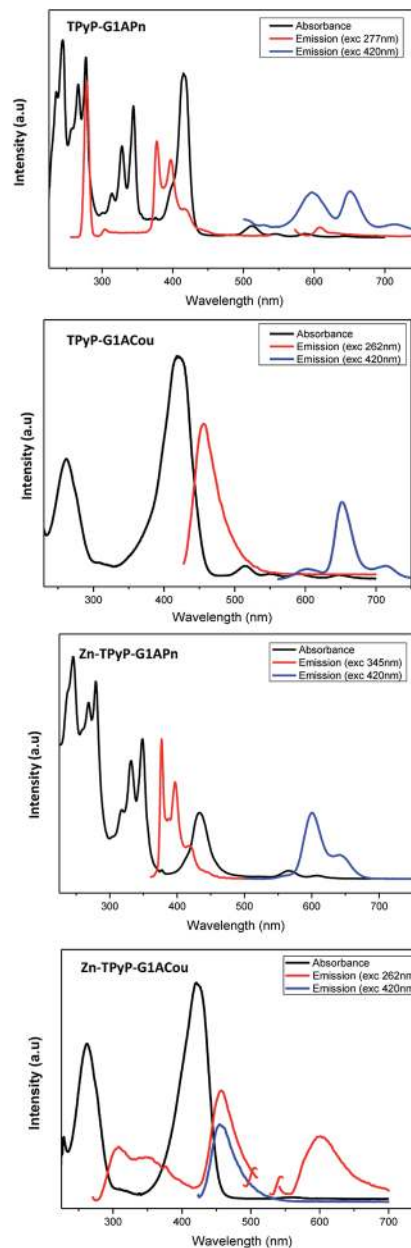

Fig. 5 Absorption and fluorescence spectra in solution (CH$_2$Cl$_2$) of pyrene and coumarin dendrimers.

In general terms, the absorption and emission spectra of supramolecular complexes in solution are, within experimental error, a combination of the spectra of the corresponding building blocks. This implies no conjugation and no energy transfer between the two chromophores, provably due to the big distance between them.

Conclusions

The synthesis simplicity and versatility of the supramolecular system based on hydrogen-bonding between a porphyrin core and carboxylic acid dendrons derived from a bifunctionalised bis(hydroxymethyl)propionic acid (bis-MPA) have been

demonstrated. The stoichiometry of the dendrimers in the condensed phase is 4 : 1, as corroborated by NMR spectroscopy.

The supramolecular architectures show mesogenic behaviour for porphyrin dendrimers of the first and second generations derived from 5-[4-(4-butoxybenzoyloxy)phenyloxy] pentanoic acid, although the flexibility of the bis-MPA units causes the formation of a calamitic superstructure and smectic mesophases are observed. Mesophase formation was not observed for porphyrin dendrimers derived from pyrene and coumarin.

Acknowledgements

References

1 D. A. Tomalia, J. B. Christensen and U. Boas, *Dendrimers, Dendrons, and Dendritic Polymers: Discovery, Applications, and the Future*, Cambridge University Press, 2012.

2 G. R. Newkome, C. N. Moorefield and F. Vögtle, *Dendrimers and Dendrons: Concepts, Syntheses, Applications*, Wiley-VCH Verlag GmbH & Co. KGaA, Weinheim, FRG, 2001.

3 S. El Kazzouli, S. Mignani, M. Bousmina and J.-P. Majoral, *New J. Chem.*, 2012, **36**, 227–240.

4 F. Vögtle, G. Richardt and N. Werner, *Dendrimer Chemistry*, Wiley-VCH Verlag GmbH & Co. KGaA, Weinheim, Germany, 2009.

5 D. Astruc, E. Boisselier and C. Ornelas, *Chem. Rev.*, 2010, **110**, 1857–1959.

6 A.-M. Caminade, D. Yan and D. K. Smith, *Chem. Soc. Rev.*, 2015, **44**, 3870–3873.

7 S. M. Grayson and J. M. J. Fréchet, *Chem. Rev.*, 2001, **101**, 3819–3868.

8 S. Campagna, P. Ceroni and F. Puntoriero, *Designing Dendrimers*, John Wiley & Sons, Inc., New Jersey, 2012.

9 K. V. Axenov and S. Laschat, *Materials*, 2011, **4**, 206–259.

10 B. Donnio, *Inorg. Chim. Acta*, 2014, **409**, 53–67.

11 Y. Wang, A. Rapakousiou, G. Chastanet, L. Salmon, J. Ruiz and D. Astruc, *Organometallics*, 2013, **32**, 6136–6146.

12 B. M. Rosen, C. J. Wilson, D. A. Wilson, M. Peterca, M. R. Imam and V. Percec, *Chem. Rev.*, 2009, **109**, 6275–6540.

13 C. Tschierske, *Angew. Chem., Int. Ed.*, 2013, **52**, 8828–8878.

14 H.-J. Sun, S. Zhang and V. Percec, *Chem. Soc. Rev.*, 2015, **44**, 3900–3923.

15 S. Hernández-Ainsa, M. Marcos and J. L. Serrano, in *Handbook of Liquid Crystals*, Wiley-VCH Verlag GmbH & Co. KGaA, 2014, DOI: 10.1002/9783527671403.hlc110.

16 M. Suárez, J.-M. Lehn, S. C. Zimmerman, A. Skoulios and B. Heinrich, *J. Am. Chem. Soc.*, 1998, **120**, 9526–9532.

17 M. Arkas and A. Papavasiliou, in *Liquid Crystals Polymers. Volume 1 – Structure and Chemistry*, ed. E. V. K. Thakur and M. Kessler, Springer, 2016, ch. 6, pp. 173–194.

18 S. Castelar, J. Barbera, M. Marcos, P. Romero, J.-L. Serrano, A. Golemme and R. Termine, *J. Mater. Chem. C*, 2013, **1**, 7321–7332.

19 M. Bucoş, T. Sierra, A. Golemme, R. Termine, J. Barberá, R. Giménez, J. L. Serrano, P. Romero and M. Marcos, *Chem.–Eur. J.*, 2014, **20**, 10027–10037.

20 J.-S. Hu, Y.-G. Guo, H.-P. Liang, L.-J. Wan and L. Jiang, *J. Am. Chem. Soc.*, 2005, **127**, 17090–17095.

21 C. M. Drain, *Proc. Natl. Acad. Sci. U. S. A.*, 2002, **99**, 5178–5182.

22 L. A. Baker and R. M. Crooks, *Macromolecules*, 2000, **33**, 9034–9039.

23 J. You, G. Li and Z. Wang, *Polymer*, 2012, **53**, 5116–5123.

24 S. R. Trenor, A. R. Shultz, B. J. Love and T. E. Long, *Chem. Rev.*, 2004, **104**, 3059–3078.

25 N. K. Mal, M. Fujiwara and Y. Tanaka, *Nature*, 2003, **421**, 350–353.

26 K. Tanaka, *Molecules*, 2012, **17**, 1408.

27 Y. Cohen, L. Avram, T. Evan-Salem and L. Frish, in *Analytical Methods in Supramolecular Chemistry*, Wiley-VCH Verlag GmbH & Co. KGaA, Weinheim, Germany, 2007, ch. 6, pp. 163–219, DOI: 10.1002/9783527610273.ch6.

28 J. Lenoble, S. Campidelli, N. Maringa, B. Donnio, D. Guillon, N. Yevlampieva and R. Deschenaux, *J. Am. Chem. Soc.*, 2007, **129**, 9941–9952.